

The Star Formation History of the Local Group Dwarf Elliptical Galaxy NGC 185. II. Gradients in the Stellar Population ¹

D. Martínez-Delgado ² and A. Aparicio

Instituto de Astrofísica de Canarias, E-38200 La Laguna, Canary Islands, Spain

Electronic mail: ddelgado@iac.es, aaj@iac.es

and

C. Gallart³

Department of Astronomy, Yale University, P.O. Box 208101, New Haven, Connecticut

06520, USA and Departamento de Astronomía, Universidad de Chile, Casilla 36-D,

Santiago, Chile

Electronic mail: carme@astro.yale.edu

Received _____; accepted _____

¹Based on observations made with the William Herschel Telescope operated on the island of La Palma by the Isaac Newton Group and with the 2.5 m Nordic Optical Telescope operated by NOT S.A. at the Spanish Observatorio del Roque de los Muchachos of the Instituto de Astrofísica de Canarias.

²Guest observer of the ING Data Centre, Cambridge, UK.

³Yale Andes Fellow.

ABSTRACT

The star formation history of the dE NGC 185, together with its spatial variations, has been investigated for old, intermediate-age, and young stars using new ground-based H_α and BVI photometry, and synthetic color–magnitude diagrams (CMDs). We find that the bulk of the stars were formed in NGC 185 at an early epoch of its evolution. After that, the star formation proceeded at a low rate until the recent past, the age of the most recent traces of star formation activity detected in the galaxy being some 100 Myr.

As for the spatial variations, the star formation rate, $\psi(t)$, for old and intermediate ages shows a gradient in the sense of taking smaller values for higher galactocentric radii. Moreover, recent star formation is detected in the central $150 \times 90 \text{ pc}^2$ only, where the youngest, 100 Myr old population is found. No traces of stars born more recently than 1 Gyr ago are found outside this central region. Since the larger concentration of stars of any age lies in the central part of a galaxy, it could be the case that the youngest stars originate from material ejected from dying stars and that this process would only be efficient enough in the center of the galaxy.

The luminous blue *stars* discovered by Baade (1951) in the center of NGC 185 are discussed using new CCD images in B and Baade’s original photographic plates. Considering their fuzzy, unresolved appearance and that a conspicuous main sequence is lacking in the CMD at our limiting magnitude, we reach the conclusion that most of Baade’s blue objects are in fact star clusters. These clusters, as well as the other stellar populations, are young (a few 100 Myr), but not as much as they would be if they were individual stars (a few 10 Myr).

A supernova (SN) remnant close to the center of NGC 185 has been analyzed from H_α images. The fact that a conspicuous MS is lacking in our CMD implies

that the SN had originated from a white dwarf progenitor.

A consistent picture arises in which the gas observed in the central region of NGC 185 would have an internal origin. The rate at which evolved stars return gas to the ISM is enough to seed the recent star formation observed in the center of the galaxy and the SN rate is probably low enough to allow the galaxy to retain the gas not used in the new stellar generations. Further support is found in the similar kinematical properties of gas and stars.

Subject headings: galaxies: dwarf — galaxies: individual (NGC 185) — galaxies: Local Group — galaxies: evolution — galaxies: photometry

1. Introduction

From the early work of Baade (1944a, 1944b), who resolved the four Andromeda dE companions into individual stars, elliptical galaxies were considered to be essentially old, coeval systems with ages comparable to those of Milky Way population II globular clusters. In the light of recent data, however, there is evidence that the majority of the Local Group dE galaxies have undergone recent star formation activity. The study of the stellar content of dE galaxies by means of their color–magnitude diagrams (CMDs) provides the most direct method of establishing whether they have had star formation episodes since the initial primeval event and even to locate in time, in a more precise way, that initial star formation event. This is the first step in correctly interpreting their integrated light by means of spectral synthesis techniques, which is the only information available at large distances. The Local Group dE galaxies offer a unique opportunity to study their evolution in detail by this means.

NGC 185 is a dE companion of the Andromeda galaxy. The presence of a dozen of bright, blue stars and two conspicuous dust patches in the central area of NGC 185 was firstly noted by Baade (1951). These “population I” features indicated that NGC 185 did not fit the concept of dE galaxies as pure population II systems and, for this reason, it was classified by Sandage & Tammann (1981) as a peculiar dE (dE3p). The possibility that a young population might exist in the center of NGC 185 was also discussed by Hodge (1963), who showed that the galaxy is bluer in the center. More recently Saha & Hoessel (1990) surveyed the variable stars, detecting about 150 RR Lyrae stars, which implies the presence of an old stellar population (older than some 10 Gyr). Recent CMDs (Lee, Freedman, & Madore 1993; Martínez-Delgado & Aparicio 1998, Paper I) showed that its bright stellar population is dominated by red giant branch (RGB) stars and a significant number of luminous red stars above the tip of the RGB (TRGB). The latter could be

an intermediate-age asymptotic giant branch (AGB) population and, together with the aforementioned population I traces, would suggest that star formation in NGC 185 has occurred over an extended period of time.

We thus have a picture of an object presumably dominated by an old population, but showing evidence of recent star formation activity. We present here the analysis of its resolved stellar content using the method based on synthetic CMDs that we have employed to study the SFHs of other Local Group dwarf galaxies (Gallart *et al.* 1996a,b; Aparicio, Gallart & Bertelli 1997a,b; Gallart *et al.* 1999). It provides a better insight into the relative contribution of the stellar population at different ages and a more complete view of its SFH.

In this paper, the SFH of NGC 185 is discussed by means of model CMDs in the light of new ground-based *BVI* CCD photometry. The wide field covered by our images allows also to study the gradients in the SFH as a function of galactocentric radius, which can yield important information to constrain dwarf galaxy formation models. In Sec. 2 we present the observations and data reduction; in Sec. 3 we discuss the young stellar population. In Sec. 4 we present our derivation of the SFH, based on synthetic CMDs, and takes into account the information provided by the bright red stars above the TRGB. In Sec. 5 we discuss the origin of the young population and the gas in NGC 185. Sec. 5 is devoted to the global properties of NGC 185. Finally, in Sec. 7 we summarize the results presented throughout the paper.

2. Observations and data reduction

The observational *VI* data of NGC 185 have been discussed in detail in Paper I. In addition, images of its central region were obtained with a Johnson *B* filter and with a narrow band H_α filter using the 2.5 m Nordic Optical Telescope (NOT) at the Roque de Los

Muchachos Observatory on the island of La Palma. The HiRAC camera with a 2048×2048 Loral CCD binned to 2×2 was used. After binning, it provides a scale of $0.22''/\text{pix}$ and a total field of $3.75 \times 3.75 (')^2$. Total integration times were 900 s in B and 1800 s in H_α . A 900 s exposure was also taken with an H_α -continuum filter. Moreover, 900 s B , 600 s V and 400 s I images were obtained of a nearby field situated $25'$ north of the center of NGC 185 to correct the foreground contamination of the broad-band images. Table 1 lists the NOT journal of observations. It has to be added to the journal of observations given in Paper I. The seeing during this campaign was excellent, with values of $\sim 0.5''$ during good part of the nights.

Bias and flat-field corrections were carried out with IRAF. DAOPHOT and ALLSTAR (Stetson 1994) were then used to obtain the instrumental photometry of the stars. Eighteen standard stars from the list of Landolt (1992) were measured during the observing run to calculate the atmospheric extinctions for each night and the equations transforming into the Johnson-Cousins standard photometric system. A total of about 180 measures in each band (B , V , and I) were used. The transformation equations are:

$$(B - b) = 25.647 + 0.023(B - V); \quad \sigma = 0.006 \quad (1)$$

$$(V - v) = 25.251 - 0.103(V - I); \quad \sigma = 0.005 \quad (2)$$

$$(I - i) = 24.557 + 0.007(V - I); \quad \sigma = 0.006 \quad (3)$$

where capital letters stand for Johnson–Cousins magnitudes and lower-case letters refer to instrumental magnitudes corrected for atmospheric extinction. The σ values are the dispersions of the fits at the barycenters of the point distribution; hence the internal zero-point errors are minimal. The dispersions of the extinction for each night vary from $\sigma = 0.009$ to $\sigma = 0.019$, and the error of the aperture corrections are of the order of 0.03.

Putting all these values together, the total zero-point error of our photometry is estimated to be about 0.04 for each band.

This calibration was used to transform our instrumental magnitudes of the comparison field into the Johnson–Cousins standard system. However, for consistency with Paper I, the B photometry of the central field of NGC 185 was calibrated using photometric data by Lee *et al.* (1993). Figure 1 shows the residuals between the magnitude of Lee *et al.* minus our instrumental magnitude, $(B_{\text{Lee}} - b)$, versus Lee *et al.* magnitude. The slope of the transformation and the color term is comparable to its dispersion, so we adopted the mean value, $B_{\text{Lee}} - b = 25.163 \pm 0.004$ to transform to Johnson–Cousins magnitudes. In addition, one standard star from Oke (1990) was observed three times to calibrate the $H\alpha$ images. The dispersion of the measures was less than 0.01 mag.

Finally, artificial star tests for the comparison field frames and for the B image of NGC 185 were performed in a similar way to that described in Paper I to obtain the *crowding-trial* table (see Aparicio & Gallart 1995), from which observational effects can be simulated in the model CMDs.

3. Recent star formation in the central region of NGC 185

3.1. The resolved young stellar population

Since reported by Baade (1951), the existence of several blue stars in the center of NGC 185, indicating a young stellar population, has been an intriguing feature of this galaxy. Hodge (1963) showed that NGC 185 is bluer in the center and that the twelve OB-type stars discovered by Baade (1951) cannot alone explain the observed blue color, suggesting that they merely are the brightest members of a population I component of $\sim 2 \times 10^5 M_{\odot}$. The photometry of this resolved blue population were published for first time by Lee *et al.*

(1993). Blue stars were also reported by Lee *et al.* (1993) who for the first time published photometry of these objects. Kim & Lee (1998) found that the color of NGC 185 gets inwardly bluer at $R < 25''$ while it remains constant outside this radius. These indications of recent star formation in the center of NGC 185 are also in agreement with the image shown in Figure 2. This image is composed of B , V , and R images obtained with the 1 m Jacobus Kapteyn Telescope (JKT) at the Roque de los Muchachos Observatory, and retrieved from the archive of the Isaac Newton Group. The blue region is confined in the central $\sim 50'' \times 30''$ of the galaxy, which corresponds to $150 \times 90 \text{ pc}^2$ at the distance of NGC 185 (616 kpc).

Unfortunately, the study of the resolved young component of NGC 185 from ground-based telescopes is extremely limited by crowding, even under good seeing conditions. Fig. 3 shows the $[(B - V), V]$ CMD of the central field of NGC 185 ($3.75' \times 3.75'$). The main structure is the *red tangle* (see Aparicio & Gallart 1994) populated by RGB and AGB stars. Besides this, a small number of blue and yellow stars are also observed with $(B - V) < 1.2$, that might be the trace of recent star formation activity. Figure 4 shows the CMD of a companion comparison field populated by stars in the range $0.4 < (B - V) < 1.4$, indicating that many of the possible young stars in the CMD of NGC 185 are probably foreground stars.

To remove the effects of the foreground contamination, we have derived the V luminosity function (LF) of the galaxy and the comparison field for stars with $0.0 < (B - V) < 1.5$ and $17 \text{ mag} < V < 23 \text{ mag}$. To select blue stars, only the stars bluer than the line defined by $V = -2.2(B - V) + 24.3$ and $V < 21$ has been considered. The star counts have been corrected of completeness using completeness factors Λ for the central region of the galaxy derived from the *crowding-trial* table discussed in Section 2. Figure 5 shows the resulting completeness-corrected LFs for NGC 185 (solid line) and the foreground field (dotted line).

While the stars with $V < 20.5$ mag in the NGC 185 field can be accounted for by foreground contamination, a significant excess of stars is observed in the range $20.5 \text{ mag} < V < 23$ mag. It is mainly produced by the clump of stars at $(B - V) \sim 1.0$ and $V \sim 21.5$ mag (Fig. 3). These stars may be young, core He-burning (HeB) intermediate-mass stars. The lack of information about the metal abundance of the young population of NGC 185 precludes an accurate determination of the age of these stars, but an approximate estimate can still be given. In Paper I, the maximum metallicity of the RGB stars was estimated to be $[\text{Fe}/\text{H}] \sim -1.1$ or $Z \sim 0.001$. Assuming a monotonic chemical enrichment, this should be a lower limit to the metallicity of the young population in the center of the galaxy. Therefore, assuming $0.001 < Z < 0.01$ for the young stars and using theoretical isochrones from the Padua library (Bertelli *et al.* 1994, and references therein), we obtain an age in the range 100–125 Myr for these stars. The $Z = 0.001$ isochrone and age 125 Myr is plotted in Figure 7.

Is the upper main sequence (MS) of a population of such an age visible in the lower, blue part of the CMD? To check this, a synthetic CMD has been computed with an SFR running from 15 to 125 Myr ago. The observational errors corresponding to the central region of NGC 185 have been simulated to produce what we will term a *model* CMD. Both, synthetic and model CMDs are plotted in Figure 6. It shows that the age of 125 Myr is consistent with conspicuous traces of the MS being absent in the CMD. If the former age estimate is correct, deeper, well sampled CMDs of the center of NGC 185 should show traces of an MS reaching $V \sim 23$ to 23.5 mag.

The CMD of the comparison field also sheds light on the nature of the yellow stars reported in Paper I populating a strip around $[(V - I), I] \sim [0.6, 21]$ to $[1.1, 17]$. The possibility was discussed there that they could be red supergiants coming from recent star formation extended over the whole galaxy. The total number of these stars found in the

NGC 185 field was 53, quite more than the 27 foreground stars predicted by the Bahcall & Soneira (1980) model of the Galaxy. However, using the counts from our comparison field after scaling to the area of the NGC 185 frame, 74 foreground stars are predicted in that region of the CMD, ruling out the possibility that significant star formation had taken place in the last 1 Gyr outside the inner region of NGC 185.

3.2. Baade’s blue stars

The dozen of luminous, blue stars in the center of NGC 185, with photographic magnitudes between 20 and 21, reported by Baade (1951), have been interpreted as impurities in a predominantly type II population. The discovery was made on photographic plates taken with the 5 m Hale Telescope at Mount Palomar (California, USA), but a finding chart was never published. These stars have played a relevant role in the evolution from the *pure population-II* concept of dE galaxies to the present view of these systems as populated in general by a mixture of old, intermediate-age and young stars. For this reason, we thought it would be interesting to go back to Baade’s original photographic plates, and Fig. 8 reproduces one of them. It must be noted that what Baade intended to say by “blue” was that the stars were brighter in the blue than in the red plates and, in any term, bluer than the general population in the field. We maintain the term “blue” here for consistency with Baade work.

From visual inspection and a comparison of the blue and red plates, we have selected 19 blue stars in the central region of NGC 185, among which the dozen blue stars mentioned by Baade should hopefully be included. It is worth noting that, also from visual inspection of the original Baade’s plates, Hodge (1973) found 17 population I stars close to the center of the galaxy. The finding chart for the 19 stars we have selected is shown in Figure 9. The positions (in pixels) of the stars in the frame and their *BVI* photometry are listed in

Table 2. Their cross-identifications with those listed by Lee *et al.* (1993) (their Table 3) are given in column 2. The stars are predominantly located in the central $\sim 20''$ (~ 60 pc) of the galaxy, within the bluer central region shown in Figure 2. Only one foreground star is expected in this area and in the corresponding region of the CMD, which confirms the idea that they belong to NGC 185.

The actual nature of these objects, marked with filled dots and pentagons in Fig. 7, is puzzling. Their location in the CMD is compatible with that of intermediate to massive, evolved He-burning stars with ages between 40 and 150 Myr (for the assumed $0.001 < Z < 0.01$ metallicity range), which is in agreement with the estimate by Lee *et al.* (1993) of the minimum age for the blue/yellow population of ~ 20 –40 Myr from the brighter stars lying along the ZAMS line. However, such a population requires the presence of an MS counterpart, which is not visible. This fact is shown in Fig. 10 where a synthetic CMD and its corresponding crowding-simulated model CMD for a stellar system with constant SFR from 1 to 40 Myr ago are plotted. Together with the MS, the model CMD of Fig. 10 shows that some bright core He-burning stars should also be observed at $V \sim 21$ mag and $(B - V) \sim 1.4$. Due to the metallicity dependency of the color indices of the bright, blue, HeB stars, less relevance has to be given to the fact that they show a diagonal sequence in the model CMD rather than a fuzzy distribution like that in the observational CMD.

Another possible interpretation of Baade’s stars is that they could be in fact be multiple stars. Our best images, with seeing $\sim 0.6''$, reveal that some of these blue objects show a fuzzy aspect and larger FWHMs. The most clear examples are objects 3 and 12 in Table 2 (see also Fig. 9), which show clear non-stellar appearances with a FWHM $> 1.5''$. At the distance of NGC 185, this corresponds to a linear size of ~ 5 pc, similar to typical sizes of Galactic open clusters, like the Pleiades or Praesepe (4 pc). Also their absolute magnitudes and colors are in the range of values of Galactic open cluster (Sagar, Joshi, &

Sinhal 1983). For comparison, the colors and magnitudes of the Pleiades, Praesepe and NGC 188 as representative of young, intermediate-age, and old open clusters, have been plotted in Figure 7.

These star clusters could be similar to those found in NGC 205 (Hodge 3, Hodge 1973; Hubble V, Da Costa & Mould 1988; Geisler *et al.* 1999), although fainter. Furthermore, Peletier (1993) and Lee (1996) has identified some bright blue objects in the central region of NGC 205, which recent *HST* images have shown to be actually stellar clusters (Cappellari *et al.* 1999; Geisler, private communication).

All these pieces of information lead us to conclude that most or all the bright blue objects found by Baade in NGC 185, are young star clusters and associations. They must be young, to account for their blue colors, but the fact that they are probably not single stars results in greater ages and lower star formation rates (SFRs). In particular, the minimum age can be estimated to be about 100 Myr, consistent with our estimated age of the latest star formation activity in NGC 185 (Section 3.1).

3.3. The star formation rate for the last 1 Gyr

The results on the number of blue and yellow stars in the CMD can be used to estimate the average SFR for the last 1 Gyr in NGC 185. This is possible due to the distributions of stars older and younger than ~ 1 Gyr being decoupled in the CMD: almost no stars older than 1 Gyr are among the blue population and almost no stars younger than that age populate the red tangle (see Gallart *et al.* 1996a).

With this aim, after subtracting the foreground star contribution, we integrated the crowding-corrected LF obtained in Sec. 3.1 to estimate the total number of blue/yellow stars. This number was then scaled to that observed in a model CMD computed with

constant star formation from 1 Gyr to 125 Myr ago and with metallicities randomly distributed in the range $0.001 < Z < 0.01$, following a method similar to that explained in Aparicio *et al.* (1997c). The resulting SFR is $\bar{\psi}_{1-0} = 6.6 \times 10^{-4} M_{\odot} \text{ yr}^{-1}$. This would be the SFR if all the blue/yellow objects were actually stars and must hence be considered as an upper value and, in any case, as a rough estimate, since no confident estimate can be made of how many of the brightest blue objects are single stars.

3.4. The emission nebula in the center of NGC 185

Gallagher, Hunter, & Mould (1984) discovered an emission nebula near the core of NGC 185. They measured $[\text{SII}]:H_{\alpha} = 1.2 \pm 0.3$ from which they concluded that it was probably a supernova remnant (SNR). Ho, Filippenko, & Sargent (1997) confirmed this result ($[\text{SII}]: H_{\alpha} = 1.5$), but classified the NGC 185’s nucleus as Seyfert 2. Young & Lo (1997) obtained the first H_{α} image of this nebula and found that its properties are compatible with those of SNRs observed in the Local Group. Finally, it has been detected neither in the VLA radio search by Dickel, D’odorico, & Silverman (1985) nor in the recent *ROSAT* HRI X-ray observations by Brandt *et al.* (1997), suggesting that it could be old (Mateo 1998).

We have obtained new H_{α} observations of the central region of NGC 185 under good seeing conditions ($\sim 0.7''$) that show the emission nebula in more detail. Figure 11 shows the continuum-subtracted H_{α} image. It is quite extended and has an arc-like morphology, suggesting that it may be a portion of a larger, old remnant. Its center is close to the nucleus of the galaxy. In addition to the nebula, two compact H_{α} objects can be seen in Fig. 11 close to the center of the galaxy. They are likely planetary nebulae and, to our knowledge, had not been previously identified. Fitting an ellipse to the shape of the partial shell of the diffuse nebula, we have estimated a diameter (D) of 80 pc as the mean of the

major and minor axes. We have measured a flux of $H_\alpha = 3.0 \times 10^{-14} \text{ erg s}^{-1} \text{ cm}^{-2}$ in very good agreement with Young & Lo (1997). For a distance of 616 kpc (Paper I), the luminosity results $L_{H\alpha} = 1.3 \times 10^{36} \text{ erg s}^{-1}$.

The evolution of an SNR is dominated by its interaction with the ISM. Although this precludes accurate dating, it is still possible to give an estimate of the age if the diameter is known and we make some assumptions on how the SNR evolves with time. Woltjer (1972) developed a simple model to describe the evolution of a SNR into a uniform-density ISM. Assuming that an SNR with a diameter of 80 pc is in its Sedov–Taylor expansion phase, (in which $t \propto D^{2.5}$), we have estimated an age of $\sim 10^5$ yr for the SNR in NGC 185.

Type Ib and II SNe are considered to be the final step of the evolution of massive, rapidly evolving stars, while type Ia SNe are thought to originate in white dwarfs in binary systems. The rate of the former, $S_{\text{Ib+II}}(t)$, can be calculated from the SFR by

$$S_{\text{Ib+II}}(t) = \int_{m_{\text{SN}}}^{\infty} \phi(m) \psi_n[t + \tau(m)] dm, \quad (4)$$

where $\phi(m)$ is the initial mass function (IMF); $\psi_n(t)$ is the SFR in units of number of stars per year; $\tau(m)$ is the life time of a star of initial mass, m , and m_{SN} is the minimum mass for type Ib and II SN progenitors. As in the remaining of the paper, the criterion is used that time increases toward the past, the present-day value being 0, whereas this criterion might seem unnatural, it is consistent with the facts that it is easier to work in terms of age, and that we do not know for sure the time at which the galaxy started its evolution. The SFR in units of number of stars is related to the SFR in mass through $\psi_n(t) = \psi(t) \times \bar{m}_\star$, with $m_\star = 0.51 M_\odot$ being the average stellar mass, obtained from integration of the Kroupa *et al.* (1993) IMF.

For NGC 185, the present day Type Ib and II SN rate should be $S_{\text{Ib+II}}(t) = 0$

because $\psi(t) = 0$ for $t < 100$ Myr, which is much more than the maximum lifetime of the progenitors. In other words, $\tau(m_{\text{SN}}) \ll 100$ Myr, which implies that the integral in (4) vanishes. For this reason, we conclude that the SNR observed in NGC 185 originates in a type Ia event. This is again consistent with the CMD: the SN having been type Ib or II would imply a conspicuous MS, even stronger than that shown in Figure 10.

In any case, it is useful to estimate the average SN rate for the recent past of the galaxy’s history as test of consistency. Let’s denote the type Ib+II rate by just $S_{\text{Ib+II}}$ and use the value $\bar{\psi}_{1-0} = 6.6 \times 10^{-4} \text{ M}_{\odot} \text{ yr}^{-1}$ obtained in Sec. 3.3 for the SFR. Assuming $m_{\text{SN}} = 10 \text{ M}_{\odot}$ and using the Kroupa *et al.* IMF, it turns out that $S_{\text{Ib+II}} = 1.76 \times 10^{-3} \bar{\psi}_{n1-0} = 2.3 \times 10^{-6} \text{ yr}^{-1}$. To this value, the type Ia SN rate, S_{Ia} , must be added to obtain the total rate. It is estimated that about 50% of the SNe in spiral galaxies are of type Ia (Tammann 1982). If this proportion is right for NGC 185 also, we would have $S_{\text{Ia}} \simeq 2.3 \times 10^{-6} \text{ yr}^{-1}$ and a total SN rate $S_{\text{tot}} \simeq 5 \times 10^{-6} \text{ yr}^{-1}$. But it could be larger considering that NGC 185 is a system with a significant intermediate to old stellar population. In any case the values obtained are compatible with only a SNR having been produced in NGC 185 in the last 10^5 yr.

4. The Star Formation History of NGC 185

While the characteristics of the recent star formation can be derived in a relatively simple way from the analysis of the CMD and other photometric and spectroscopic information, tracing out the SFH for old and even intermediate-age epochs is by far more complicated. The analysis based upon synthetic CMDs computed for different input SFHs opens a way to the determination of the SFH for these older ages. In CMDs such as that used for NGC 185 in this paper, old stars are observed in the red tangle, together with many intermediate-age stars, if present. The bright stars frequently found over the TRGB in CMDs of dE galaxies may help to discriminate between the old and intermediate-age SFH.

These stars are probably AGBs with masses over $\sim 1 M_{\odot}$ and are hence intermediate-age, or possibly even young (younger than ~ 1 Gyr).

Bright AGBs have acquired a high relevance as tracers of intermediate-age stars in dE galaxies (*e.g.*, see Freedman 1992 and Han *et al.* 1997 for early and later examples). For this reason we will first discuss to what extent the presence of such an intermediate-age stellar population in NGC 185 can be qualitatively deduced from the distribution of bright AGBs. After that we will make the full analysis of the SFH based on synthetic CMDs and we will discuss their galactocentric gradients.

4.1. AGB stars as tracers of the intermediate-age population

In our $[(V - I), I]$ CMD (see Paper I), a considerable number of bright stars are observed above the TRGB. These kinds of stars have been observed optically from the ground in the inner regions of all four Andromeda dE companions and have several times been interpreted as bright AGBs and as the signature of an intermediate-age population. Nevertheless, Martínez-Delgado & Aparicio (1997) have shown that the severe crowding in the central regions of these galaxies would make the RGB stars appear brighter than they are, mimicking the intermediate-age AGB population ⁴. For this reason, we will restrict the following analysis to the less crowded regions of the galaxy with $a > 177''$ (where a is the semimajor axis of the concentric ellipses centered on the galaxy, as defined in Paper I).

In order to shed light on the nature of this population and for illustrative purposes, we

⁴It must in any case be noted that the absence of the bright AGB feature in the CMD is not enough to rule out the possibility of a significant intermediate-age population (see the case for LGS3, Aparicio *et al.* 1997b; or Phoenix, Martínez-Delgado, Gallart, & Aparicio 1999).

have compared the observed CMD with three model CMDs computed with constant $\psi(t)$ for different age intervals (see Sec. 4.2). Observational effects for the $177'' < a < 236''$ have been simulated using the procedure explained in Paper I. Figure 12 displays the observed CMD for this region and the model CMDs for the different age intervals.

The explicit and realistic simulation of the observational effects performed in these model CMDs implies that we can directly compare their visual aspect, as well as the star counts, to those of the observed CMD. A simple visual inspection indicates that the model CMD for the 15–9 Gyr old population (Fig. 12a) cannot by itself alone account for the presence of the stars brighter than $I \sim 20.5$ mag but that some intermediate-age population is needed. Since some of those stars could also be foreground stars, we have counted the stars in a region situated above the TRGB with $19 \text{ mag} < I < 20 \text{ mag}$ and $1.2 < (V - I) < 4.2$ in the CMD of NGC 185 and in a companion field. The results for several elliptical annuli of NGC 185 (N_{AGB}) and for the comparison field (N_{f}) after scaling to the corresponding areas, are given in Table 3. The errors listed in this table have been calculated assuming Poissonian statistics. Table 3 shows that the foreground contribution is not enough to account for the number of stars observed in the CMD of NGC 185 in any of the $a > 177''$ annuli, supporting the idea that an intermediate-age population is required. This is not in contradiction with the result by Geisler *et al.* (1999), who report *HST* observations of an inner and an outer region of NGC 185 in which upper-AGB stars are absent (see Sec. 4.3). This result could be due to the small field of the *HST* Planetary Camera ($36.8 \times 36.8''^2$). Indeed, using this and our results listed in Table 3, only four stars are expected above the TRGB in the interval $19 \text{ mag} < I < 20 \text{ mag}$, $1.2 < (V - I) < 4.2$ for the outer field of Geisler *et al.*

4.2. Method and hypotheses

The detailed derivation of the SFH from synthetic CMDs requires deeper data than those we have available for NGC 185 (see Gallart *et al.* 1999). However an estimate of the old, intermediate-age and young SFR is still possible from our CMD of the galaxy. We have followed the method described by Aparicio *et al.* (1997b). In short, the SFH is considered to be composed of three functions: the SFR, $\psi(t)$, the IMF, $\phi(m)$, and the chemical enrichment law, $Z(t)$. A function $\beta(f, q)$ accounting for the fraction and mass distribution of binary stars can also be considered (see Gallart *et al.* 1999). The functions $\phi(m)$, $Z(t)$ and $\beta(f, q)$ are treated as input information to the models. Several combinations of them can be checked. For each of them, the best solution or a group of good solutions are obtained for $\psi(t)$, in the following way. First, several simple *partial* models are obtained for the combination of $\phi(m)$, $Z(t)$ and $\beta(f, q)$. Each partial model contains stars in a given, relatively narrow age interval with constant SFR. *Global* models can then be computed by linear combinations of the partial models in the form $\psi(t) = l \sum a_i \psi_i$, where ψ_i is the SFR of partial model i , a_i is the linear combination coefficient and l is a normalization constant. Secondly, several regions are defined in the CMD sampling areas populated by stars of different ages and in different stellar evolution phases, and the numbers of stars in these regions in the observational CMD and in each of the partial models are counted. The star counts corresponding to any of the global model can be then computed and compared with those of the observational CMD through a merit function. Finally, the best or a group of good global models is found out by minimization of the merit function with respect to the a_i coefficients. This procedure gives several solutions for the SFH producing model CMDs compatible with the observational one. The solution is not unique, but the range covered by them indicates the uncertainty of the result and allows the elimination of impossible scenarios for the SFH.

In the particular case of NGC 185, data are not deep enough to seek a detailed description of the SFH. For this reason we intend to find out only estimates of the old, intermediate and young SFH and therefore, we have simplified the number of inputs for $\phi(m)$, $Z(t)$ and $\beta(f, q)$. In particular, we have used only one shape for $\phi(m)$: the one by Kroupa *et al.* (1993) and we have neglected the effects of binary stars. The later is justified by the fact that we are dealing mainly with evolved RGB and AGB stars. For them, only binaries with $q \simeq 1$ can noticeably affect the distribution of stars in the CMD. This is because, in other case, binaries in which the least massive component is in the RGB or AGB have likely a massive component having evolved into the white dwarfs phase, while binaries with the most massive component in the RGB or AGB have probably a secondary in the low MS, thereby very weakly affecting the total luminosity of the system.

In spite of the age–metallicity degeneracy in the RGB phase, limits can be set on $Z(t)$ if two simple assumptions are made: that no stars can exist in the galaxy with metallicities implying a red tangle different (in shape, wideness or position) from the observed one, and that $Z(t)$ is not a decreasing function of time. With these assumptions, three *partial* model CMDs with the same constant SFR were computed for three age intervals (in Gyr): $1 \leq t < 3$, $3 \leq t < 9$, and $t \geq 9$, (see for example Fig. 12). Stars in each partial model have been computed with metallicities taken at random inside an interval such that the position and the full width of the red tangle are matched. In this way, independently of the age distribution resulting for global model, the restriction that the position and shape of the red tangle must be well reproduced will be satisfied. Of course, other choices of $Z(t)$ could also (but not always) produce good results if combined with adequate $\psi(t)$. However, the low time resolution that we can achieve implies that the task of looking for those solutions is not justified. Since low time resolution means averaging $\psi(t)$ for long intervals of time, we believe that the solution obtained here is a good approximation to reality.

The comparison between model and observed CMDs is made through star counts in the three selected regions defined in Figure 13. These regions were chosen to sample those stellar evolutionary phases that are sensitive to the distribution of stellar ages that can be most efficiently discriminated with our data. In particular, region 1 would be populated by old and intermediate-age RGB and AGB stars; region 2 would contain old and intermediate-age AGB stars; and region 3 would be populated by bright, intermediate-age AGB stars only.

4.3. The resulting SFH

As discussed in Paper I, the CMD of the inner regions of NGC 185 is strongly affected by crowding. For this reason, we have divided our study in two parts. For the inner $177''$ (semimajor axis; see Paper I for the definition of several annular elliptical regions in NGC 185), a simple estimate of the total averaged $\psi(t)$ has been obtained from the number of stars in the upper part of the red tangle (Aparicio, Bertelli, & Chiosi 1999). This estimate has been made from two annular regions: i) inner-A ($a < 118''$) and ii) inner-B ($118'' \leq a < 177''$). The resulting SFRs are $\bar{\psi}_{\text{tot}} = 8.2 \times 10^{-3} \text{ M}_{\odot} \text{ yr}^{-1}$ or $\bar{\psi}_{\text{tot}}/A = 3.3 \times 10^{-8} \text{ M}_{\odot} \text{ yr}^{-1} \text{ pc}^{-2}$ for region inner-A and $\bar{\psi}_{\text{tot}} = 4.6 \times 10^{-3} \text{ M}_{\odot} \text{ yr}^{-1}$ or $\bar{\psi}_{\text{tot}}/A = 1.9 \times 10^{-8} \text{ M}_{\odot} \text{ yr}^{-1} \text{ pc}^{-2}$ for region inner-B.

For the outer ($177'' \leq a$) regions the analysis of the SFH has been done as described in Sec. 4.2 for three elliptical annular regions defined as follows (see Paper I): i) outer-A ($177'' \leq a < 236''$); ii) outer-B ($236'' \leq a < 295''$); and iii) outer-C, ($295'' \leq a$). The latter includes the two outer annuli defined in Paper I.

The observed CMDs of the outer regions are displayed in Figure 14. In these CMDs, a number of blue stars (bluer than $(V - I) \sim 1.4$) and brighter than $I \sim 22$ mag are present.

From estimates made from the foreground field CMD shown in Fig. 4 (see Sec. 3.1), these stars are very probably foreground stars and will not be further considered in SFH analysis.

The main result arising from our analysis is that the bulk of the stellar population of NGC 185 formed at an early epoch, but that star formation has continued at a lower rate for almost the rest of the lifetime of the galaxy. Figure 15 shows the adopted solutions for $\psi(t)$. Each of them has been obtained averaging the global models matching the stellar counts of the observational CMD to better than 1.5σ . The results are also listed in Table 4, together with the estimates for the inner regions. The SFR for young stars in the innermost region obtained in Sec. 3.3 has been also included. The SFR values for each age interval listed in the first four lines have been used to obtain the averaged SFRs for the complete period of star formation ($\bar{\psi}_{15-1}$) given in line 5. Lines 6 to 10 give the same as lines 1 to 5, after normalization to the area of the region in pc^2 .

Our results for the SFH can be compared with deeper *HST* observations. Geisler *et al.* (1999) present preliminary results for the field-star CMDs for two regions in the vicinity of the NGC 185 globular clusters FJJIII (*inner* field) and FJJIV/V (*outer* field). Both diagrams show a striking red clump (RC) and a small number of blue horizontal branch (HB) stars. The outer field of Geisler *et al.* falls inside our outer region-A. We have explicitly computed the model CMD resulting from the SFH we have obtained for this region, but simulating it to be ~ 3 mag deeper than our observational CMD. The resulting model CMD is shown in Figure 16 and represents what would be obtained from deep *HST* observations if our results for the SFH are correct. The visual, qualitative agreement with the *HST* CMD of the FJJIV/V field (Geisler, private communication) is very good, especially in the HB and RC morphology but also regarding the width and overall structure of the RGB. It must be noted that the RC [$(V - I) \sim 1.1$; $I \sim 24.0$] of the model CMD shown in Fig. 16 is mainly populated by intermediate-age stars. Consequently,

the RC obtained from *HST* data is a good alternative observational confirmation of the star formation having taken place at intermediate ages in NGC 185, as has been found in our analysis.

4.4. Galactocentric gradients of the SFR

The values given for $\bar{\psi}_{\text{tot}}/A$ in the last line of Table 4 indicate a gradient of decreasing SFR with galactocentric radius. We have studied how this variation is correlated with the surface brightness (SB) profile of NGC 185, in order to search for possible gradients of the mass-to-light ratio within the galaxy. These would in turn indicate gradients in the composition of the stellar population, and hence in the shape of the SFH.

Figure 17 shows the variation of $\log(\bar{\psi}_{\text{tot}}/A)$ as a function of galactocentric radius (filled dots) together with the same for the mean SB μ_r (open circles) obtained after averaging the μ_r profile by Kent (1987) for each annulus. Both quantities follow a similar trend which can be interpreted as the relative amounts of stars of different ages being similar for each region. This is in good agreement with the relatively small changes in the shape of $\psi(t)$ obtained for the outer regions, and the fact that it can reasonably be extended inward indicates that, overall, shape would have been similar in the inner regions too. This could be in apparent contradiction with the young population having been found close to the center of the galaxy only, but this may be compensated by the fact that the total life-averaged $\psi(t)$ is also bigger for the innermost region.

5. Young stars and the origin of the gas in NGC 185

The origin of the raw gas from which the young stars are born in E and dE galaxies is a puzzling question. Although E galaxies were long thought to be devoid of gas, Faber

& Gallagher (1976) showed that the mass returned during the galaxies’ lifetimes to the interstellar medium by evolved, dying stars should be significant. However, it is found that the H I in E galaxies is highly extended with respect to the optical components and is rotating with angular momenta per unit mass much higher than that of the stars. This points to an external origin for the gas in these systems (van Gorkom 1992).

The case may be different for dE. Young & Lo (1997) find different scenarios for the three dEs they analyze: no gas in NGC 147; gas having different angular momentum per unit mass from stars in NGC 205 and gas kinematically compatible with that of the stellar component in NGC 185. For the latter, in particular, they find a velocity dispersion $\sigma_v = 15.3 \text{ km s}^{-1}$ for the gas, somewhat smaller than the stellar one: $\sigma_v = 22 \text{ km s}^{-1}$ (Bender *et al.* 1991). The results for the SFH we have obtained in the previous sections can shed light on the question of the external or internal origin of the gas in NGC 185.

The rate at which the material is returned to the ISM by dying stars in the central region of NGC 185 can be evaluated from integration of the SFR through

$$R(t) = \int_{m_1}^{m_u} [m - p(m)] \phi(m) \psi[t + \tau(m)] dm$$

,

where m_1 and m_u are lower and upper limits, respectively, for the stellar mass and $p(m)$ is the mass of the remnant of a star of initial mass m . Note that within this paper the criterion is used that time increases toward the past and the present day value is 0. Using $\psi(t) = 8.2 \times 10^{-3} \text{ M}_\odot \text{ yr}^{-1}$ for $1 \text{ Gyr} \leq t < 15 \text{ Gyr}$ and $\psi(t) = 6.6 \times 10^{-4} \text{ M}_\odot \text{ yr}^{-1}$ for $0 \text{ Gyr} \leq t \leq 1 \text{ Gyr}$, and the relations given by Vassiliadis & Wood (1993) for $p(m)$, we obtain for the present time $R(0) = 10^{-3} \text{ M}_\odot \text{ yr}^{-1}$, which is 1.5 times the recent, averaged SFR $\bar{\psi}_{1-0}$. It is worth noting that no significant differences are found if the integration is stopped at $t = 0.1 \text{ Gyr}$, and that almost 90% of the returned material comes from stars born in the $15 \text{ Gyr} \leq t < 1 \text{ Gyr}$ interval.

Making a detailed kinematical evolutionary model is beyond the scope of this paper, but some other pieces of information can be qualitatively evaluated. The gas content observed in the central region of NGC 185 ($7.3 \times 10^5 M_{\odot}$) can be built up in about 2 Gyr from the ejected gas not used for star formation. But for this picture to work it is also necessary that SN explosions and high-velocity winds from massive stars are neither efficient enough to sweep away the ISM nor to heat it up over shorter time-scales. Lozinskaya (1992) shows that one SN of energy 10^{51} erg would transfer some 5×10^{49} erg to the interstellar medium. But this energy represents only 10% of the kinetic energy of the gas in NGC 185 (Young & Lo 1997). As we have shown, this amount of energy would be injected into the ISM at a rate of once every 5×10^5 yr. On the other hand, Chevalier (1974) showed that the cooling time-scale for typical SNR is of the order of 10^5 to 10^6 yr, likely short enough to allow NGC 185 maintaining the cool gas component it shows.

Summarizing, we have a picture in which the kinematical properties of gas and stars are consistent with the internal origin of the former. The rate at which evolved stars return gas to the ISM is enough to seed the recent star formation observed in the center of the galaxy and the SN rate is probably low enough to allow the galaxy to retain the gas not used in the new stellar generations.

Another puzzling question is why NGC 147, a galaxy that could be considered similar to NGC 185, with a large amount of old, dying stars, shows traces of neither gas nor recent star formation (see Young & Lo 1997 for the gas and Han *et al.* 1997 for the stellar population). Resolving this question will require a more detailed analysis of the properties of NGC 147 and could perhaps indicate that mechanisms such as gas removing by SN explosions and subsequent delay of star formation would be at work (see Burkert & Ruiz-Lapuente 1997).

6. Global properties of NGC 185

The SFR $\psi(t)$ can be used together with the distance obtained in Paper I and data from other authors, to calculate integrated properties of NGC 185. Table 5 gives a summary of these properties. Bracketed figures refer to the bibliographic sources for each data. The first two lines list values for $\psi(t)$ averaged for several intervals of time: $\bar{\psi}_{15-0}$ is the average for the whole life of the galaxy; $\bar{\psi}_{1-0}$ corresponds to the last 1 Gyr. As the field covered by our observations is smaller than the galaxy size ($R_t = 16'$, Hodge 1963), the resulting SFR has been multiplied by a scale factor obtained as the rate between the total luminosity of the galaxy (Sandage & Tammann 1981) and the luminosity covered by our field estimated from the surface-brightness profile given by Kent (1987). Lines 3 and 4 give the same values normalized to the area. Line 5 gives the $\bar{\psi}_{1-0}/A$ value obtained for the central region in which the recent star formation is detected, in which area is $A_{\text{inner}} = 150 \text{ pc} \times 90 \text{ pc}$ (see Sec. 3.1).

The distance to the Milky Way and to the barycenter of the Local Group are given afterwards, followed by the absolute magnitudes and the total luminosities in different bands, calculated for the adopted distance. M_\star is the mass in stars and stellar remnants, calculated from integration of $\psi(t)$ and assuming that a fraction 0.8 of this integral remains locked into stellar objects. To obtain M_{gas} , the H I mass has been multiplied by 4/3 to account for the He content. μ is the gas fraction relative to the total mass intervening in the chemical evolution. Finally, the gas and total mass to luminosity fractions are given.

7. Conclusions

The SFH and the properties of the dE galaxy NGC 185 have been analyzed in the light of new ground-based H_α and BVI photometry. The SFH has been estimated for old,

intermediate-age, and young stars and its spatial variations investigated using synthetic CMDs, detailed simulation of observational effects and reliable estimates of the foreground stellar contamination.

The recent star formation is confined into the central $150 \times 90 \text{ pc}^2$ of the galaxy. After correction for foreground star contamination, the $[(B - V), V]$ CMD of the central field ($3.75' \times 3.75'$) shows a population of blue/yellow stars that indicates star formation in the last 1 Gyr. The youngest stars were probably formed some 100 to 125 Myr ago and the SFR since 1 Gyr ago is estimated to be $\bar{\psi}_{1-0} = 6.6 \times 10^{-4} \text{ M}_{\odot} \text{ yr}^{-1}$.

The luminous blue stars discovered by Baade (1951) in the center of NGC 185 have been discussed using new B CCD images and Baade's original photographic plates. A total of 19 blue, bright objects have been found from a visual inspection of these plates in the central $20''$ of the galaxy. We believe that most of these objects are the blue, bright stars originally mentioned by Baade. We have ruled out the possibility that they are foreground stars. They lie in a region where evolved, core He-burning, 40 to 150 Myr old stars are expected, but, if this were their age range, they should be accompanied by a conspicuous MS, which is not present. Based on this and on the fact that several of them show a fuzzy, unresolved aspect, with an FWHM larger than the stellar one, we conclude that most of these objects are young stellar clusters. In fact, at the distance of NGC 185, their linear sizes, color and absolute magnitudes are consistent with those of typical young Galactic open clusters.

We have presented new H_{α} images of the central region of the galaxy showing the SNR discovered by Gallagher *et al.* (1984) with more detail. It has an arclike morphology and might be a portion of a larger, old remnant 80 pc in diameter. We estimate its H_{α} luminosity to be $1.3 \times 10^{36} \text{ erg s}^{-1}$ and its age $\sim 10^5 \text{ yr}$. Assuming that it proceeded from an SN II, we estimate the SFR in the central region to be in the range 3×10^{-3} to

$6 \times 10^{-3} M_{\odot} \text{ yr}^{-1}$, almost one order of magnitude larger than the recent SFR estimated from the resolved young population. Again, this would likely require a conspicuous MS to be present in the CMD and hence compels us to conclude that the SNR comes from an SN Ia progenitor.

We have analyzed the SFH for two inner and three outer regions in NGC 185 using synthetic CMDs and an empirical simulation of observational effects using the results of a large number of artificial-star tests. The resulting scenario shows that the bulk of the stars in NGC 185 were formed in an early epoch. The star formation has continued at a much lower rate for intermediate ages. This produces a population of stars above the TRGB. They are relatively bright AGBs and cannot be accounted for by foreground contamination. No traces of star formation more recent than 1 Gyr are found outside the central region of the galaxy, where the star formation continued until some 100 Myr ago. The absence of younger stars could be interpreted as the star formation proceeding in small, mild bursts, taking place with intervals of several 100 Myr between them.

New stars are produced only in the very central region of the galaxy. This could indicate that young stars are born from processed material ejected by old, dying stars. Calculations show that the rate at which evolved stars return gas to the ISM is enough to seed the recent star formation observed in the center of the galaxy and the SN rate is probably low enough to allow the galaxy to retain the gas not used in the new stellar generations. This, together with the fact that the kinematical properties of gas and stars are similar, supports the idea of an internal origin for the gas component observed in the central regions of the galaxy.

Finally, we have derive several integrated global parameters of NGC 185 which are listed in Table 5.

We are indebted to Dr. Allan Sandage for useful indications of which objects probably Dr. Baade referred to as being *the blue stars* in the Baade's original plates of NGC 185. We thank the enjoyable and interesting discussions, and his patience teaching us how to look at the plates, and making possible to obtain some useful reproductions of them. The Observatories of the Carnegie Institution of Washington are also acknowledged for making available to us Baade's original plates of NGC 185 taken with the 5 m Hale Telescope at Mount Palomar, California (USA). We also thank to the anonymous referee for careful reading of the original manuscript and for useful comments and suggestions. We are indebted to Dr. Geisler for useful comments and for making available to us his preliminary *HST* results on NGC 185. This work has been substantially improved after fruitful discussions with Drs. Bertelli, Chiosi, Da Costa, Gordon, Freedman, Ho, Welch and Young to whom we are very grateful. AA thanks the Observatories of the Carnegie Institution and its staff at Pasadena for their hospitality during his one year term stay as a visiting researcher. During that period, AA was funded by the Dirección General de Enseñanza Superior, Investigación y Desarrollo of the Kingdom of Spain (Grant PB95-554). DMD also thanks the staff of the Observatories of the Carnegie Institution at Pasadena for their hospitality during his visit. This work is part of the PhD thesis of DMD and has been financially supported by the Instituto de Astrofísica de Canarias (Grant P3/94) and the Dirección General de Enseñanza Superior, Investigación y Desarrollo of the Kingdom of Spain (Grant PB94-0433).

REFERENCES

- Aparicio, A. 1999, in The stellar content of the Local Group, Proceeding of the IAU Symp. 192, ed. Whitelock & Cannon, in press
- Aparicio, A., Bertelli, G., & Chiosi, C. 1999, in preparation
- Aparicio, A., & Gallart, C. 1994 in ESO Conference and Workshop Proceedings No 51, The Local Group: Comparative and Global Properties, edited by A. Layden, R.C. Smith & J. Storm. (Garching, ESO), p. 115
- Aparicio, A., & Gallart, C. 1995, AJ, 110, 2105
- Aparicio, A., Gallart, G., & Bertelli, G. 1997a, AJ, 114, 669
- Aparicio, A., Gallart, G., & Bertelli, G. 1997b, AJ, 114,680
- Aparicio, A., Dalcanton, J. J., Gallart, C. & Martínez-Delgado, D. 1997c, AJ, 114, 1447
- Baade, W. 1944a, ApJ, 100, 137
- Baade, W. 1944b, ApJ, 100, 147
- Baade, W. 1951, Publ. Obs. Univ. of Michigan, No. 10, 7
- Bahcall, J. N. & Soneira, R. M. 1980, ApJS, 44,73
- Bertelli, G., Bressan, A., Chiosi, C., Fagotto, F., & Nasi, E. 1994, A&AS, 106, 275
- Bender, R., Paquet, A., & Nieto, J. L. 1991, A&A, 246, 349
- Brandt, W. N., Ward, M. J., Fabian, A. C. & Hodge, P. W. 1997, MNRAS, 291,709
- Burkert, A. & Ruiz-Lapuente, P. 1997, ApJ, 480, 297
- Cappellari, M., Bertola, F., Burstein, D., Buson, L. M., Greggio, L. & Renzini, A. 1999, ApJ, in press
- Chevalier, R. A. 1974, ApJ, 188, 501

- Da Costa, G. S., & Mould, J. R. 1988, ApJ, 334, 159
- Dickel, J. R., D'odorico, S. & Silverman, A. 1985, AJ, 90, 414
- Faber, S. M. & Gallaguer, J. S. 1976, ApJ, 204, 365
- Ford, H.C., Jenner, D. C., & Epps, H. W. 1973 ApJ, 183, L73
- Freedman, W. L. 1992, AJ, 104, 1349
- Gallagher III, J. S., Hunter, D. A., & Mould, J. R. 1984, ApJ, 281, L63
- Gallart, C., Aparicio, A. & Bertelli, G. 1996a, AJ, 112, 1950
- Gallart, C., Aparicio, A. & Bertelli, G. 1996b, AJ, 112, 2596
- Gallart, C., Freedman, W. L., Aparicio, A., Bertelli, G. & Chiosi, C. 1999, AJ, submitted
- Geisler, D., Armandroff, T., Da Costa, G., Lee, M. G. & Sarajedini, A. 1999, in The stellar content of the Local Group, Proceeding of the IAU Symp. 192, ed. Whitelock & Cannon, in press
- van Gorkom, J. 1992, in Morphological and Physical Classification of Galaxies, ed. G. Longo *et al.* (Dordrecht:Kluwer), 233
- Han, M., Hoessel, J. G., Gallaguer, J. S., Holtzman, J. & Stetson, P. B. 1997, AJ, 113, 1001
- Ho, L. C., Filippenko, A. V. & Sargent, W. L. W. 1997, ApJS, 112, 315
- Hodge, P. W. 1963, AJ, 68, 691
- Hodge, P. W. 1973, ApJ, 182, 671
- Kent, S. M. 1987, AJ, 94, 306
- Kim, S. C. & Lee, M. G. 1998, Journal of the Korean Astronomical Society, 31, 51
- Kroupa, P., Tout, C. A., & Gilmore, G. 1993, MNRAS, 262, 545
- Landolt, A. U. 1992, AJ, 104, 340

- Lee, M. G. 1996, AJ, 112, 1438
- Lee, M. G., Freedman, W. L., & Madore, B. F. 1993, AJ, 106, 964
- Lorinskaya, T. A. 1992, *Supernovae and Stellar Wind in the Interstellar Medium* (New York:AIP)
- Martínez-Delgado, D., & Aparicio, A. 1997, ApJ, 480, L107
- Martínez-Delgado, D., & Aparicio, A. 1998, AJ, 115, 1462 (Paper I)
- Martínez-Delgado, D., Gallart, C. & Aparicio, A. 1999, AJ, August 1999, in press
- Mateo, M. 1998, ARA&A, 36, 445
- Oke, J. B. 1990, AJ, 99,1621
- Peletier, R. F. 1993, A&A, 271, 51
- Sagar, R., Joshi, U. C., Sinvhal, S. D. 1983, Bull. Astr. Soc. India, 11, 44
- Sage, L. J., Welch, G. A. & Mitchell, G. F. 1998, ApJ, 507, 726
- Saha, A., & Hoessel, J. G. 1990, AJ, 99, 97
- Sandage, A., & Tammann, G. A. 1981, *A Revised Shapley-Ames Catalog of Bright Galaxies* (Carnegie Institution of Washington, Washington DC)
- Stetson, P. B. 1994, PASP, 106,250
- Tamman, G. A. in *Supernovae: A survey of Current Research*, ed. N. J. Rees and R. J. Stoneham (Boston:Reidel), p 371
- Vassiliadis, E. & Wood, P. R. 1993, ApJ, 413, 641
- Young, L. M., & Lo, K. Y. 1997, ApJ, 476, 127
- Woltjer, L. 1972, ARA&A, 10, 129

Fig. 1.— Residuals of the transformation to standard B magnitudes using the photometry of Lee *et al.* (1993).

Fig. 2.— Color image of the central region of NGC 185 obtained from a combination of B , V and R images. The size of the field is $2.8' \times 2.8'$. North is up and east is to the left.

Fig. 3.— $[(B - V), V]$ CMD of the central ($3.75' \times 3.75'$) region of NGC 185.

Fig. 4.— $[(B - V), V]$ CMD of a comparison field situated $25'$ north of the center of NGC185.

Fig. 5.— Crowding-corrected V luminosity function for blue–yellow stars in NGC 185 (solid line) and in the comparison foreground field (dotted line).

Fig. 6.— Synthetic (*panel A*) and model (*panel B*) CMDs computed with constant star formation rate $\psi(t)$ for the interval of time from 15 to 0.125 Gyr ago. Stellar metallicities take random values in the interval $0.001 \leq Z \leq 0.01$.

Fig. 7.— $[(B - V), V]$ CMD of the central ($3.75' \times 3.75'$) region of NGC 185. An isochrone from the Padua library (Bertelli *et al.* 1994) for $Z=0.001$ and age 125 Myr is overplotted. Baade’s blue *stars* are displayed as large dots, with pentagon shaped ones being those showing an unresolved appearance. The position in the CMD of the Pleiades (open triangle), Praesepe (open square), and NGC 188 (open circle) Galactic open clusters at the distance and reddening of NGC 185 are also plotted.

Fig. 8.— Magnification of the central part of photographic plate number PH662B of NGC 185 taken by W. Baade in 1952 August 20/21 with the Palomar 200" telescope. A 103a0 emulsion was used with a GG1 filter. The exposure time was 30 minutes. North is up and east is to the left. The size of the field is $3.2' \times 3.2'$. Baade wrote in the plate cover: *Incipient resolution in photographic light clearly visible*. This plate is published for the first time here.

Fig. 9.— Finding chart for the 19 blue stars selected from the original Baade plates in the central region of NGC 185 listed in Table 2. The seeing is $0.6''$. North is up and east is to the left. The size of the field is $2.5' \times 2.5'$.

Fig. 10.— Synthetic (*panel A*) and model (*panel B*) CMD, computed with constant $\psi(t)$ for the interval of from 1 to 0.04 Gyr ago. Stellar metallicities take random values in the interval $0.001 \leq Z \leq 0.01$.

Fig. 11.— Continuum-subtracted H_α image of the center of NGC 185. The exposure time is 900 s. North is up and east is to the left. The size of the field is $2.3' \times 2.3'$. The cross marks approximately the center of the galaxy. The two compact objects close to the center are possible previously unknown planetary nebulae. The three similar-looking objects visible at the periphery of the figure are planetary nebulae catalogued by Ford *et al.* (1973).

Fig. 12.— Comparison of the observed CMD for the annulus $177'' \leq a < 236''$ (upper panel) with partial model CMDs for three age intervals (lower panels). The figure suggests that the bright red stars above the TRGB of the observational diagram are probably intermediate-age AGB stars, which is confirmed by subsequent investigation of the SFH.

Fig. 13.— The regions used for the determination of the SFH overplotted onto the CMD of the outer regions ($a > 177''$) of NGC 185.

Fig. 14.— Observed $[(V - I), I]$ CMDs for the three regions in which the outer part of NGC 185 has been divided for the analysis of the SFH (see text for details).

Fig. 15.— SFRs of regions outer-A, outer-B and outer-C as a function of time.

Fig. 16.— Model CMD produced by the SFH shown in Fig. 15 (*top panel*) for a limited magnitude about 3 mag deeper than that reached by our photometry. This is approximately

what would be seen from deep *HST* observations if our results for the SFH are correct.

Fig. 17.— Radial variation for the $\log(\bar{\psi}/A)$ compared with the SB profile of NGC 185 obtained by Kent (1987) averaged for each annulus.

Table 1. Journal of observations

Date	Object	Time(UT)	Filter	Exp. time (s)	FWHM (")
97.07.27	NGC 185	03:43	H_{α} -cont	900	0.7
97.07.27	NGC 185	03:59	H_{α}	900	0.7
97.07.27	NGC 185	04:14	H_{α}	900	0.7
97.07.29	NGC 185	04:37	B	900	0.6
97.07.29	FIELD	04:55	I	400	0.5
97.07.29	FIELD	05:02	V	600	0.5
97.07.29	FIELD	05:13	B	900	0.6

Table 2. Baade’s blue stars in NGC 185

N	N_{Lee}	X	Y	B	V	I	$(B - V)$	$(V - I)$	FWHM ($''$)	Note
1	-	108.37	346.03	21.56	21.14	20.55	0.42	0.59	0.7	
2	3802	171.98	291.21	21.63	20.96	19.37	0.67	1.59	1.4	a
3	-	220.05	283.78	19.90	19.55	-	0.35	-	1.8	a
4	3116	221.23	260.47	20.20	19.79	-	0.41	-	0.7	
5	2244	229.66	215.15	21.70	21.01	20.07	0.69	0.94	1.1	a
6	2468	245.62	228.42	21.40	20.92	19.18	0.48	1.74	1.2	a
7	2452	251.97	228.17	21.80	20.67	19.39	1.13	1.28	-	
8	2588	251.58	235.00	21.78	21.48	-	0.30	-	-	a
9	-	243.85	254.91	20.80	20.00	-	0.80	-	-	a
10	-	253.21	248.88	20.98	20.90	-	0.08	-	-	b
11	2933	252.93	252.16	21.01	20.22	19.30	0.79	0.92	-	a
12	1839	276.22	193.54	21.25	20.66	19.62	0.59	1.04	2.5	a
13	-	263.20	242.87	21.92	20.89	19.32	1.03	1.57	-	ab
14	5370	277.79	380.95	21.26	20.36	19.58	0.90	0.78	0.7	c
15	-	273.01	264.95	21.70	20.72	19.33	0.98	1.39	-	ab
16	3095	285.02	260.89	21.30	21.24	20.64	0.06	0.60	-	ab
17	4084	306.23	309.79	21.28	20.78	19.86	0.50	0.92	1.2	a
18	1369	373.77	169.53	20.78	20.46	20.12	0.32	0.34	0.6	
19	5683	325.68	406.92	21.69	21.25	20.92	0.44	0.33	0.6	

^aFuzzy, unresolved appearance.

^bImmersed in a dust cloud, possibly with high reddening.

^cPlanetary nebula.

Table 3. AGB stars and contamination by foreground stars

	N_{AGB}	N_{f}
$177'' < a < 236''$	28 ± 5	7 ± 3
$236'' < a < 295''$	27 ± 5	7 ± 2
$295'' < a < 354''$	15 ± 4	5 ± 2
$a > 354''$	11 ± 3	5 ± 2

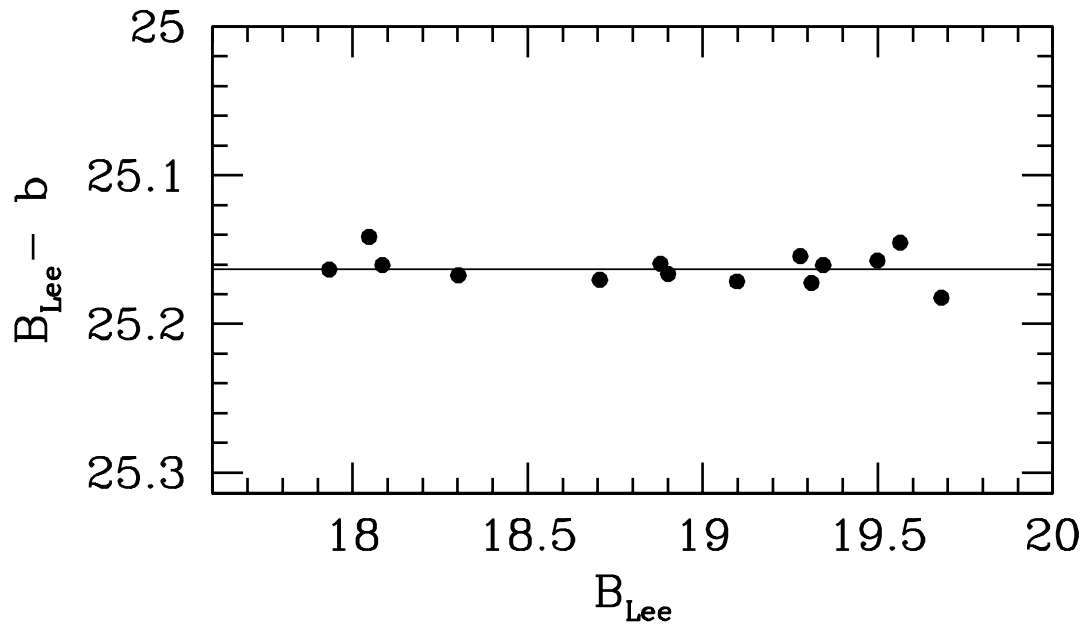
Table 4. Star formation rates

	Inner A	Inner B	Outer A	Outer B	Outer C
$\bar{\psi}_{15-9}$ ($10^{-4} \text{ M}_{\odot}\text{yr}^{-1}$)	-	-	23.3	13.2	16.0
$\bar{\psi}_{9-3}$ ($10^{-4} \text{ M}_{\odot}\text{yr}^{-1}$)	-	-	1.0	3.7	1.7
$\bar{\psi}_{3-1}$ ($10^{-4} \text{ M}_{\odot}\text{yr}^{-1}$)	-	-	3.7	1.5	0.5
$\bar{\psi}_{1-0}$ ($10^{-4} \text{ M}_{\odot}\text{yr}^{-1}$)	6.6	-	-	-	-
$\bar{\psi}_{tot}$ ($10^{-4} \text{ M}_{\odot}\text{yr}^{-1}$)	82	46	11.0	7.5	7.7
$\bar{\psi}_{15-9} / A$ ($10^{-9} \text{ M}_{\odot}\text{yr}^{-1}\text{pc}^{-2}$)	-	-	8.7	4.4	3.2
$\bar{\psi}_{9-3} / A$ ($10^{-9} \text{ M}_{\odot}\text{yr}^{-1}\text{pc}^{-2}$)	-	-	0.4	1.2	0.3
$\bar{\psi}_{3-1} / A$ ($10^{-9} \text{ M}_{\odot}\text{yr}^{-1}\text{pc}^{-2}$)	-	-	1.4	0.5	0.1
$\bar{\psi}_{1-0} / A$ ($10^{-9} \text{ M}_{\odot}\text{yr}^{-1}\text{pc}^{-2}$)	2.6	-	-	-	-
$\bar{\psi}_{tot} / A$ ($10^{-9} \text{ M}_{\odot}\text{yr}^{-1}\text{pc}^{-2}$)	33	19	4.1	2.5	1.5

Table 5. Global properties of NGC 185

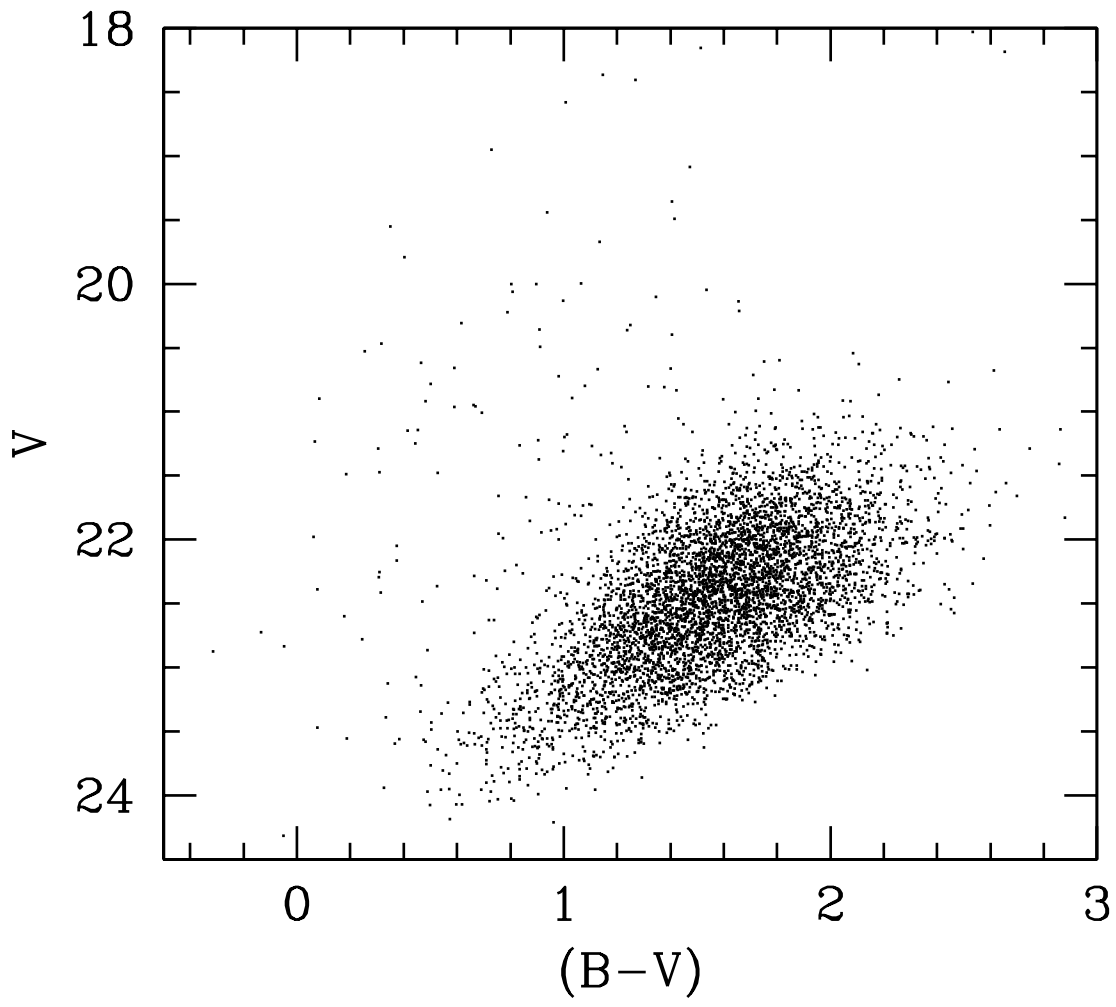
		NGC 185
$\bar{\psi}_{15-0}$	$(10^{-4} \text{ M}_{\odot}\text{yr}^{-1})$	247 (1)
$\bar{\psi}_{1-0}$	$(10^{-4} \text{ M}_{\odot}\text{yr}^{-1})$	6.6 (1)
$\bar{\psi}_{15-0}/A$	$(10^{-9} \text{ M}_{\odot}\text{yr}^{-1}\text{pc}^{-2})$	1.22 (1)
$\bar{\psi}_{1-0}/A$	$(10^{-9} \text{ M}_{\odot}\text{yr}^{-1}\text{pc}^{-2})$	0.03 (1)
$\bar{\psi}_{1-0}/A_{\text{inner}}$	$(10^{-9} \text{ M}_{\odot}\text{yr}^{-1}\text{pc}^{-2})$	49 (1)
d	(Mpc)	0.616 (1)
d (LG)	(Mpc)	0.178 (1)
M_B		-14.63 (2)
M_V		-15.52 (3)
L_B	(10^8 L_{\odot})	1.40
L_V	(10^8 L_{\odot})	1.25
M_{\star}	(10^8 M_{\odot})	2.96 (1)
M_{gas}	(10^8 M_{\odot})	0.0073 (4,5)
$\mu = M_{\text{gas}}/(M_{\star} + M_{\text{gas}})$		0.025 (1)
M_{gas}/L_V	$(\text{M}_{\odot}/\text{L}_{\odot})$	0.006

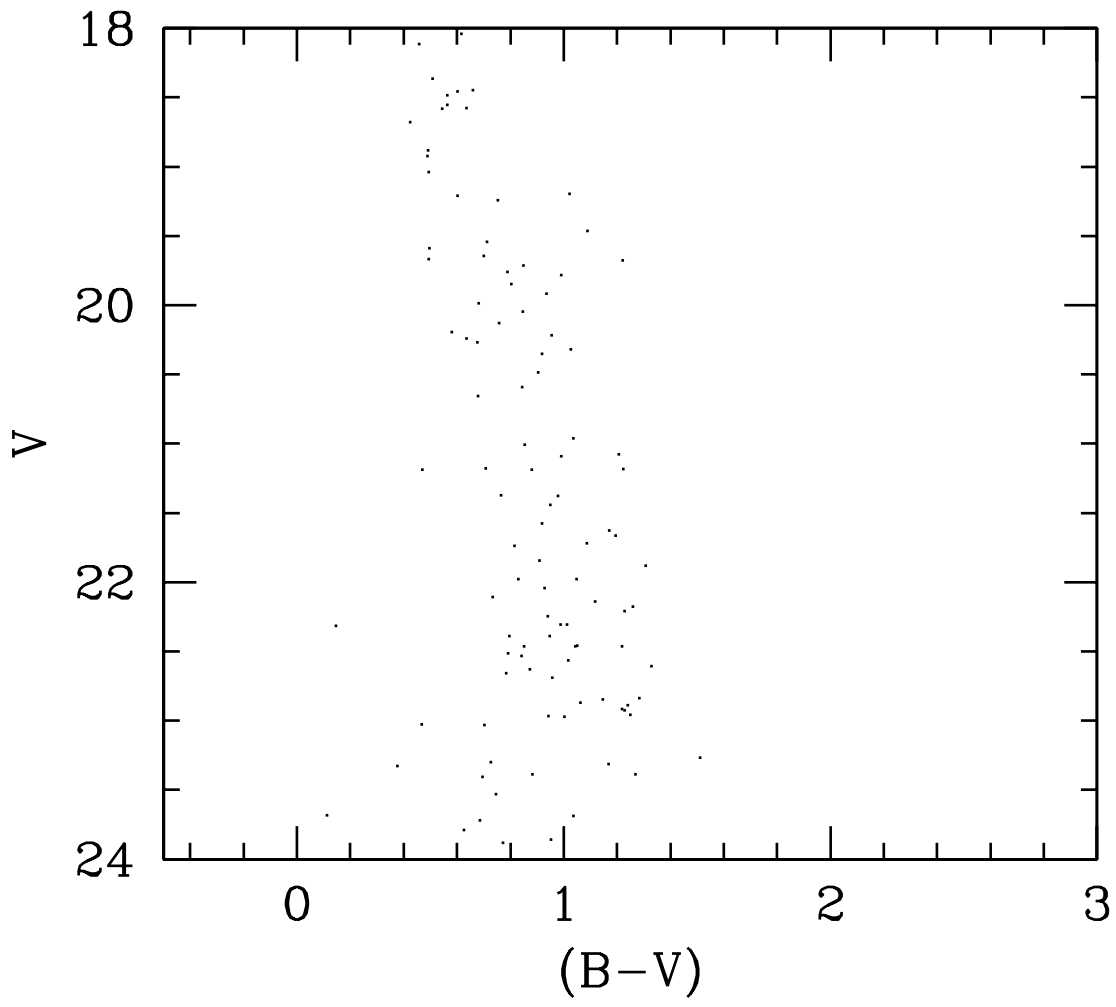
References. — (1) This paper; (2) Sandage & Tammann 1987; (3) Kodaira *et al.* 1987; (4) Young & Lo 1997; (5) Sage, Welch & Mitchell 1998

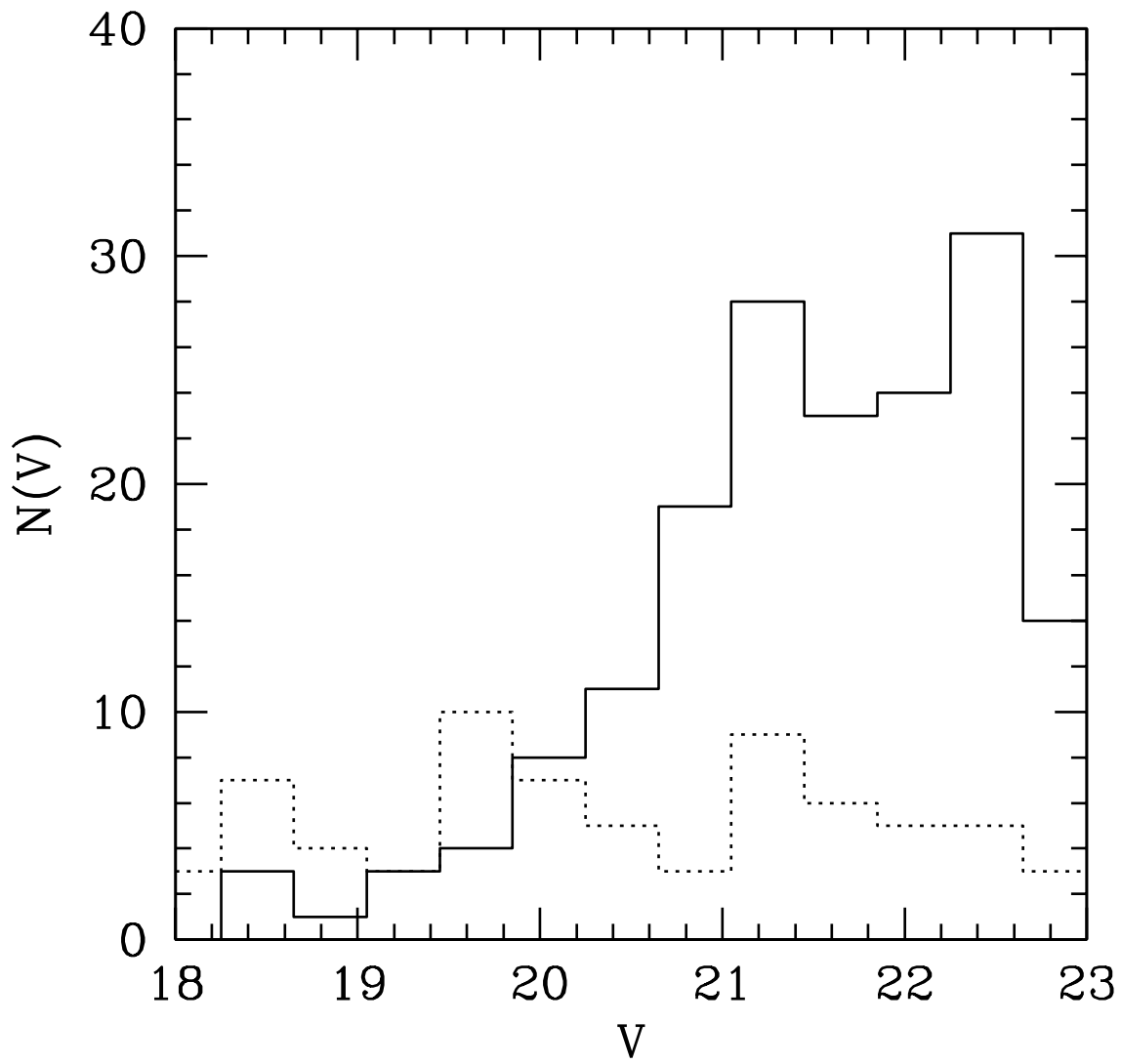


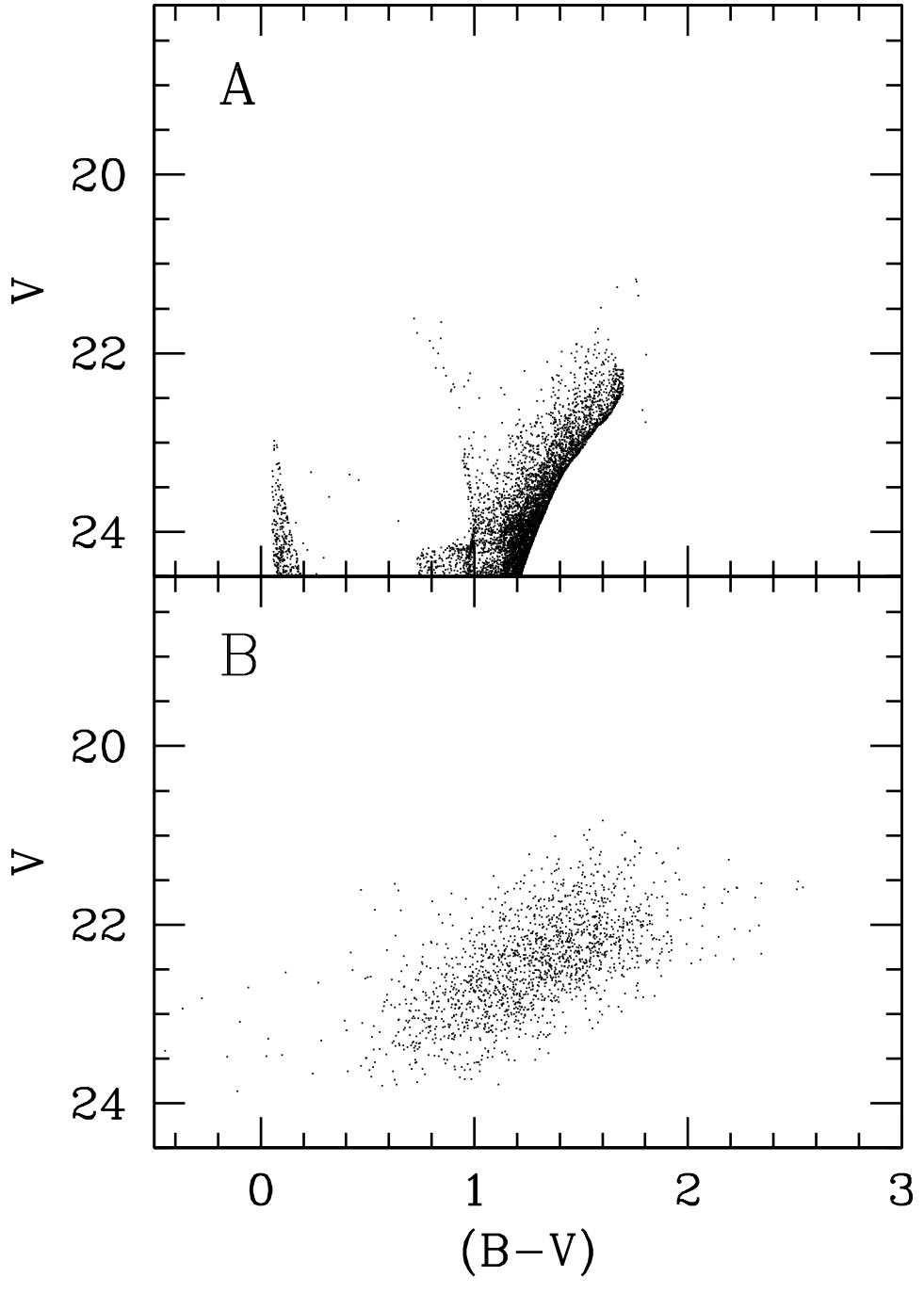
This figure "md.fg2.jpg" is available in "jpg" format from:

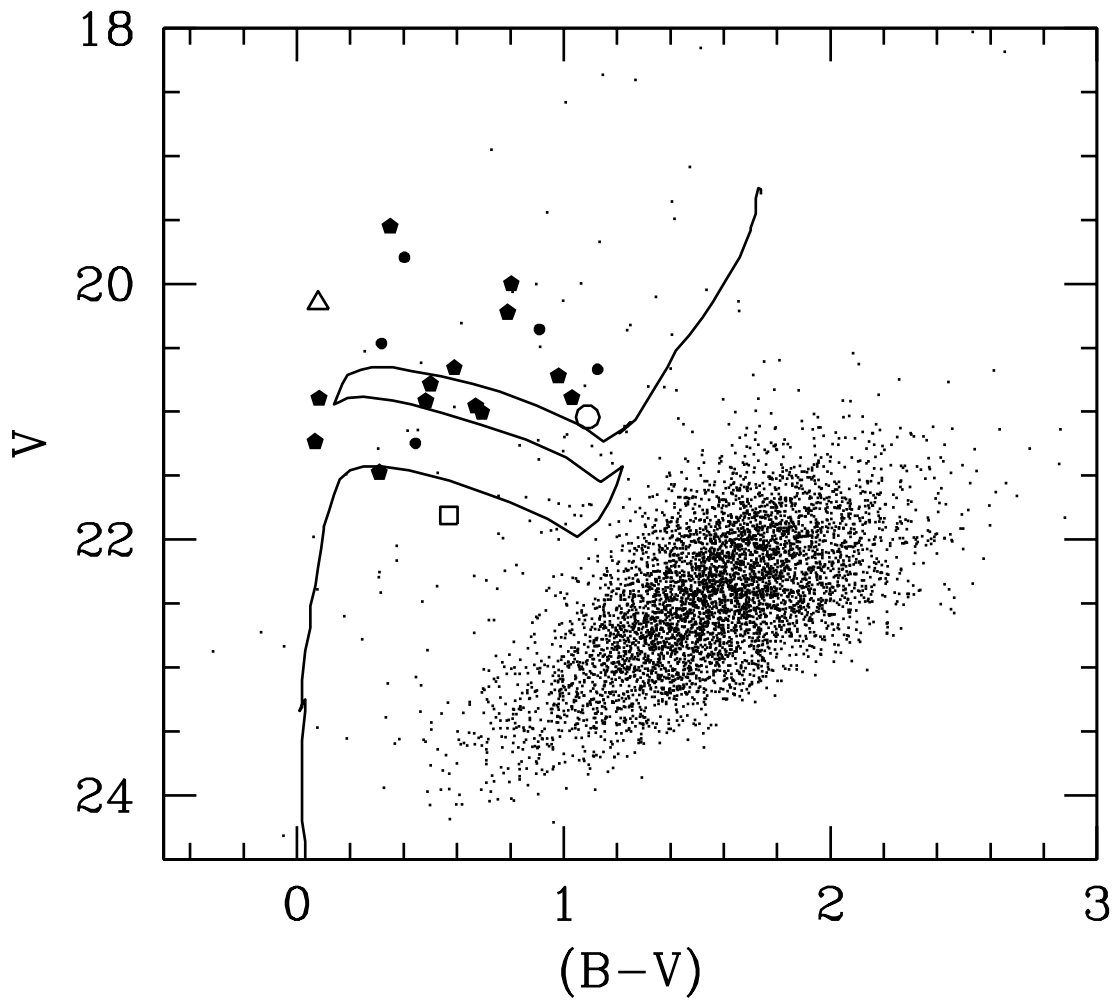
<http://arxiv.org/ps/astro-ph/9907049v1>









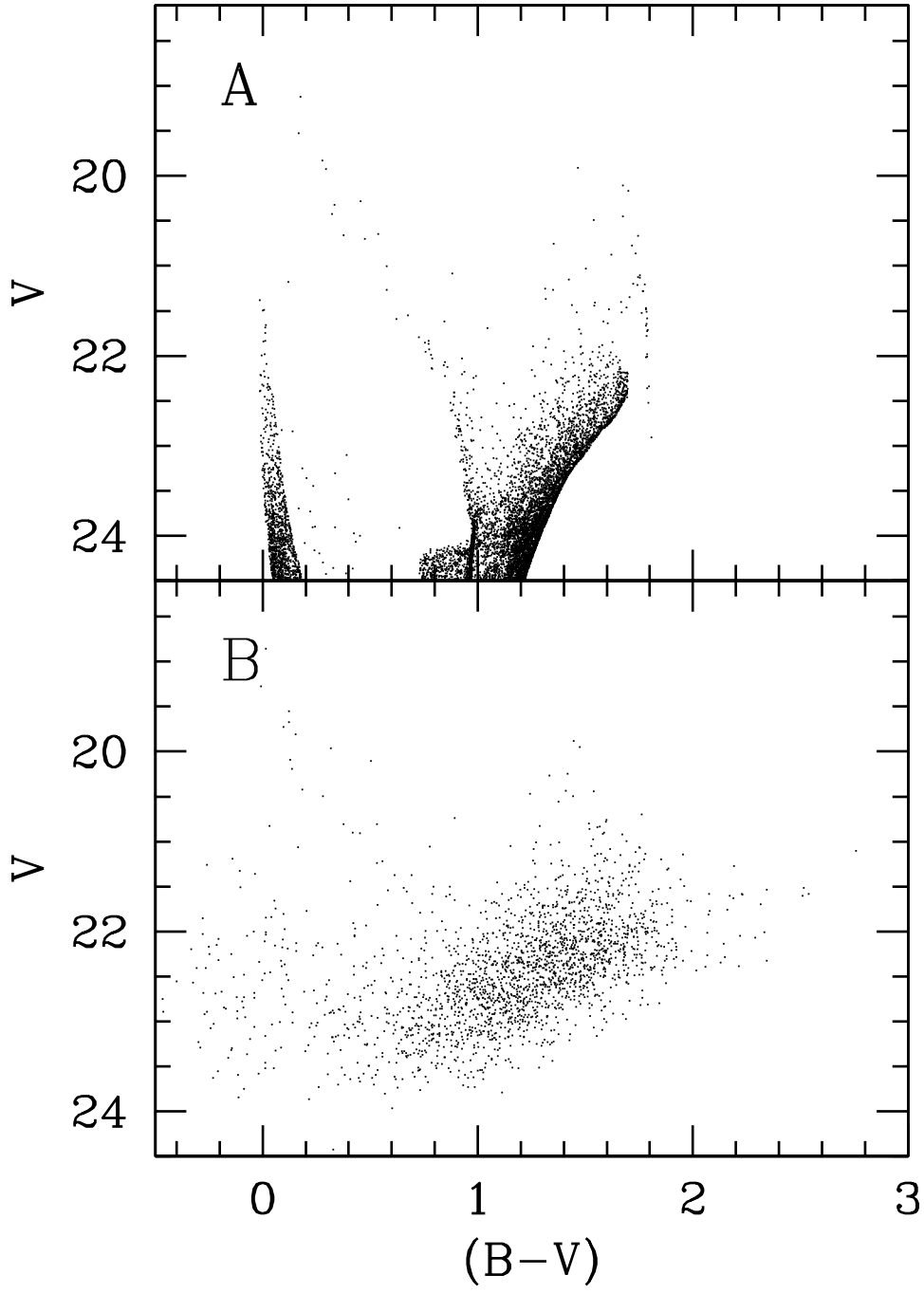


This figure "md.fg8.jpg" is available in "jpg" format from:

<http://arxiv.org/ps/astro-ph/9907049v1>

This figure "md.fg9.jpg" is available in "jpg" format from:

<http://arxiv.org/ps/astro-ph/9907049v1>



This figure "md.fg11.jpg" is available in "jpg" format from:

<http://arxiv.org/ps/astro-ph/9907049v1>

177 " < a < 236 "

